

ReViT: Enhancing Vision Transformers with Attention Residual Connections for Visual Recognition

Anxhelo Diko^a, Danilo Avola^a, Marco Cascio^{b,a} and Luigi Cinque^a

^aDepartment of Computer Science, Sapienza University of Rome, Via Salaria 113, Rome, 00198, Italy, Italy

^bDepartment of Law and Economics, University of Rome UnitelmaSapienza, Piazza Sassari 4, Rome, 00161, Italy, Italy

ARTICLE INFO

Keywords:

Vision Transformer
Feature Collapse
Self-attention Mechanism
Residual Attention Learning
Visual Recognition

ABSTRACT

Vision Transformer (ViT) self-attention mechanism is characterized by feature collapse in deeper layers, resulting in the vanishing of low-level visual features. However, such features can be helpful to accurately represent and identify elements within an image and increase the accuracy and robustness of vision-based recognition systems. Following this rationale, we propose a novel residual attention learning method for improving ViT-based architectures, increasing their visual feature diversity and model robustness. In this way, the proposed network can capture and preserve significant low-level features, providing more details about the elements within the scene being analyzed. The effectiveness and robustness of the presented method are evaluated on five image classification benchmarks, including ImageNet1k, CIFAR10, CIFAR100, Oxford Flowers-102, and Oxford-IIIT Pet, achieving improved performances. Additionally, experiments on the COCO2017 dataset show that the devised approach discovers and incorporates semantic and spatial relationships for object detection and instance segmentation when implemented into spatial-aware transformer models.

1. Introduction

Nowadays, automatic visual recognition systems have become increasingly popular as powerful support tools for a wide range of vision-related applications, e.g., object detection and tracking [4, 9], image analysis and classification [42], or scene segmentation [37] and understanding [10]. Such systems have been developed to mimic the remarkable human brain ability to perfectly correlate low-level visual features (e.g., edges, color, or shapes) and semantic-level information for perceptual identification and recognition tasks [1, 2]. In the past decade, deep learning algorithms have been extensively employed to model how the human brain processes visual information since artificial neural networks are inspired by the structure and function of biological neurons; indeed, they can analyze visual data learning to recognize patterns and features in images [27]. Precisely, the understanding of visual content has been revolutionized by Convolutional Neural Networks (CNNs), primarily because of their ability to analyze an image split into smaller patches, extract multi-scale localized features, and synthesize them to generate highly expressive representations [21, 19]. Despite this, due to its limited receptive field, the convolutional operation of standard CNNs cannot recognize long-range dependencies, such as arbitrary relationships among distant image regions. To address this limitation and facilitate the handling of long-range dependencies in visual tasks, several architectures based on transformers have emerged [7, 33]. Notably, the traditional transformer neural network initially gained popularity in the field of natural language processing [34]. This popularity stemmed from its self-attention mechanisms, which enable the modeling of extensive dependencies between tokens within a sequence of data, overcoming the limitation of CNNs. Additionally, in contrast to CNNs, specifically engineered for visual tasks with pre-existing knowledge and incorporating inductive biases such as locality and translation equivariance [8], ViT adopts an approach where an image is treated as a sequence of patches. This different architectural choice leads to a deficiency in such inductive biases, making ViT less effective at generalizing when trained on smaller datasets [7]. Nevertheless, it has been observed that the training scale can override the need for strong inductive biases, showcasing the substantial potential of transformers when trained on extensive datasets [7, 8, 33].

Standard ViT models are characterized by their deep architecture, comprising multiple sequential computational blocks. Each of these blocks consists of a self-attention layer, a multi-layer perceptron (MLP), and a residual connection

✉ diko@di.uniroma1.it (A. Diko); avola@di.uniroma1.it (D. Avola); cascio@di.uniroma1.it (M. Cascio); cinque@di.uniroma1.it (L. Cinque)

ORCID(s):

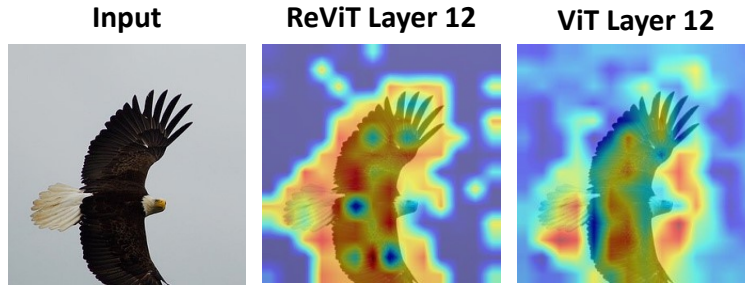


Figure 1: Illustration of feature maps learned from ReViT and ViT obtained using GradCAM [31] algorithm.

that bypasses the self-attention layer. This hierarchical structure necessitates multiple consecutive passes to process the input token sequence and compute scene representations. While the input token sequence traverses deeper layers of the network, tokens tend to become highly similar to each other. This phenomenon leads to a loss of feature diversity, commonly referred to as feature collapsing. The main contributing factor to this phenomenon is the global nature of the self-attention mechanism and its tendency to combine features across patches [32]. Specifically, as token processing progresses through the network’s deeper layers, the generated attention maps become increasingly global, aggregating features between patches at a global scale and losing their focus on local information [7, 8]. This shift from local awareness causes the network to forget low-level features and only emphasize global characteristics. While the ability to capture global context is a desirable trait of transformers, considering low-level cues such as shape and color, typically found in shallower network layers, can be advantageous for vision-related tasks like image classification and object detection. In addition to the globality issue, ViT architectures are also considered less robust at translation invariance compared to CNNs [16, 7]. This limitation makes ViTs less reliable in real-world scenarios where objects may appear in varying positions and sizes.

Inspired by the shortcomings observed in the ViT architecture and insights from neuroscience, which suggest that the human brain transmits visual information through a sequential hierarchical process from simple to specialized cells via the aggregation of electrical impulses [15], we present the Residual Attention Vision Transformer (ReViT)¹. This innovative network architecture introduces an attention residual learning technique, enhancing the performance of visual recognition tasks by integrating low-level information from shallow to deeper network layers and contrasting the over-globalization of the attention mechanism. Specifically, given standard vision transformer blocks, attention information is passed between consecutive layers and integrated with the attention information of the current layer using a permutation invariant aggregation function. This connection facilitates the transmission and accumulation of attention-related information from shallower to deeper layers, enabling the ability to identify low-level features while preserving the original ability of transformers to extract global context. Consequently, by empowering the attention mechanism with the ability to capture such features, the resulting learned representations are expected to exhibit greater feature diversity. Additionally, since low-level features like color and shape can be useful in identifying objects in a scene regardless of their position and size, this mechanism improves the translation invariance of ViT. In order to assess the efficacy of incorporating residual attention into ViT (i.e., ReViT), we conducted a comprehensive empirical analysis. Our evaluation spanned five image classification benchmarks, namely ImageNet1K [30], CIFAR-10 [18], CIFAR-100 [18], Oxford Flowers-102 [28], and Oxford-IIIT Pet [29]. The results demonstrated significant performance enhancements when using ReViT compared to the original ViT counterpart approach in all datasets. Furthermore, due to their high image quality, we employed the Oxford Flowers-102 and Oxford-IIIT Pet datasets to highlight ReViT superiority over ViT in image classification tasks involving translation invariance, such as horizontal and vertical shifts, as well as scale invariance. These experiments provided quantitative evidence of ReViT advantages in handling these scenarios. Moreover, we quantitatively analyze the global spread of the attention map in ViT and ReViT models employing the non-locality metric [8] and show that our approach can preserve more local information than ViT. Apart from our quantitative evaluations, we conduct a qualitative analysis by comparing the feature maps learned by ViT and ReViT models employing the GradCAM [31] algorithm to visually demonstrate how ReViT excels in integrating low-level features into its learned representations, as depicted in Fig. 1. Finally, we established that the proposed

¹<https://github.com/ADiko1997/ReViT>

residual learning strategy can seamlessly integrate into multiscale transformer architectures like the Multiscale Vision Transformer v2 (MViTv2) [20] and the Shifted-window transformer (Swin) [24], verifying its effectiveness in various tasks, including image classification on ImageNet1K, object detection, and instance segmentation on COCO2017 [23], obtaining improved performances.

In summary, the major contributions of this paper are:

1. To the best of our knowledge, a novel ViT-based architecture has been introduced that uses residual attention modules capable of incorporating important low-level visual characteristics into the learned representation while maintaining the ability to extract global context, thereby enhancing feature diversity throughout deeper network layers.
2. We conduct an extensive experimental phase to showcase the effectiveness of the proposed model in image classification on benchmarks like ImageNet1K, CIFAR-10, CIFAR-100, Oxford Flowers-102, and Oxford-IIIT Pet.
3. Empirically demonstrate that residual attention enhances the robustness of ViT against translation invariance through a comprehensive evaluation in the context of image classification tasks on the Oxford Flowers-102 and Oxford-IIIT Pet datasets.
4. Thoroughly analyze the global spread of attention maps, with and without residual attention, using the non-locality metric.
5. We qualitatively analyze the learned feature maps of ViT and ReViT models using the GradCAM algorithm to examine the attention mechanism's ability to integrate low-level features into acquired representations in the presence of residual attention.
6. We evaluate our module's seamless integration into multi-scale architectures using MViTv2 and Swin with residual attention on ImageNet1K for image classification and COCO2017 for object detection and instance segmentation.

The rest of this paper is organized as follows. Section 2 introduces relevant work that inspired this study. Section 3 comprehensively describes important background information and the proposed method. Section 4 describes the experiments performed to validate the proposed approach quantitatively and qualitatively. Section 5 reports an ablation study on the residual attention. Finally, Section 6 draws some conclusions from this study.

2. Related Work

2.1. Vision Transformers

In visual recognition tasks, standard CNN-based models are currently the most powerful algorithms for image analysis [14, 35]; even so, these networks are designed to capture short-range dependencies using small convolutional filters that only look at small image patches at a time. However, due to its self-attention mechanisms, which have been very successful for natural language processing, the transformer architecture was recently applied to process images, capturing long-range dependencies between image patches, thus allowing the handling of complex visual relationships better. Therefore, the ViT [7] neural model was introduced, splitting the image into a grid of patches fed through a stack of transformer blocks, which use self-attention to encode the global relationships between the different patches. To enhance ViT capabilities, Touvron et al. [33] proposed the Data-efficient Image Transformers (DeiT) using a knowledge distillation technique that transfers the knowledge learned by a larger teacher model to a smaller student model (the DeiT model) during training. This helps to improve the generalization performance of ViT. Despite the promising results, extracting low-level image features becomes a significant challenge. To address such an issue, Han et al. [11] introduced a new kind of neural architecture that divides image patches into sub-patches and later employs an extra transformer block to analyze their relationship. For the same reason, Liu et al. [24] presented the Swin transformer, a multiscale architecture operating in local windows with a shifted window policy to extract spatial cross-window relationships between patches. Moreover, in literature, several works proposed enhancing local feature representations by aggregation strategy [39] and integrating local and global attention layers [5, 22]. Aiming to extract features at different levels of granularity and resolution, Li et al. [20] proposed the MViTv2 to capture local and global image features using a hierarchical architecture with multiple scales, which can improve the model ability to define and recognize objects within a scene in different sizes and orientations. Differently, to improve the performance of ViT-based models for large-scale image classification, Wang et al. [36] introduced the kNN search inside the attention mechanism to reduce the impact of noisy or irrelevant features by exploiting the locality of patches to extract meaningful

information, thus resulting in overall better feature representation. Finally, Yu et al. [38] proposed the Bilateral Local Attention vision Transformer (BOAT) based on an attention mechanism that integrates the common image-space local attention with feature-space local attention. The latter can compute attention among relevant image patches even if they are not close to each other within the image plane. Therefore, this type of attention is a natural compensation to image-space local attention, which may miss capturing meaningful relationships between existing patches across different local windows. However, kNN-based and BOAT models require significant computational resources, limiting their practical applicability.

Due to their success in increasing CNNs capabilities, ViT and all its variants include residual connections. However, their usual application does not completely solve the feature collapsing of ViT in deeper layers. Therefore, addressing such an issue, we propose residual attention learning for vision transformers, which propagates attention among adjacent transformer blocks while preserving the computational load, improving feature diversity and performances in tasks like image classification, object detection, and instance segmentation.

2.2. Feature Diversity

Traditional downstream ViT models are characterized by deep architectures, resulting in reduced feature diversity as the depth increases. This limitation hampers their ability to represent information effectively. While variants of ViT that have similarities to CNNs, e.g., MViTv2 or Swin, are less affected by this issue, it should be considered that they are primarily designed for image-specific tasks, deviating from the original ViT goal of achieving generalization across a wide range of tasks and modalities. Consequently, addressing this challenge is essential for enhancing the representational capabilities of standard ViT models and promoting consistency in hardware and software designs across various tasks and modalities. To tackle this problem, Tang et al. [32] found inspiration from residual connections, which aids in maintaining a degree of feature diversity. They propose an augmented shortcut scheme that enhances the flow of information from low-level layers to deeper layers through multiple parallel alternative paths. These shortcuts are essentially parametrized linear projection sequences that bypass the attention mechanism within the transformer block. This augmentation significantly boosts feature diversity as the information travels through the deeper layers of ViT. In contrast, d'Ascoli et al. [8] introduced a novel attention layer called the gated positional attention layer. When equipped with a soft inductive bias to mimic the behavior of CNNs, this layer improves the feature diversity of ViT models. However, these methods either require the addition of extra parameters or alterations to the standard ViT workflow by changing the composition of the transformer block. For these reasons, the proposed method offers an elegant solution. It increases feature diversity in ViT architectures by forwarding attention among transformer layers with minimal additional parameters and seamlessly integrating into the original ViT workflow. Additionally, contrary to [32], the proposed method addresses the issue of feature diversity by contrasting attention over-globalization, which is the main catalyst in feature collapsing rather than propagating past features.

3. Background and Methodology

3.1. Vision Transformer Layer

The standard ViT adopts the typical architecture as proposed in [34] with MLP and attention modules alternatively stacked throughout the network. Among different types of attention mechanisms, scaled dot-product self-attention is the most used one. It enables the model to extract complex relationships among the elements in the input data sequence and to dynamically assign varying significance degrees to each element according to the learned relationships [34]. Formally, given a set of image patch features $X = \{x_1, x_2, x_i, \dots, x_N\}$, with $X \in \mathbb{R}^{N \times C}$, where x_i is the vector representation of the i -th image patch, N is the total number of patches, and C is the channel size of the image, a learnable linear projection layer is used to generate query Q , key K , and value V vectors, such that $Q, K, V \in \mathbb{R}^{N \times d}$ with d being the projection dimensionality. Afterward, for a given attention layer l , the dot product between queries and keys is computed and scaled by the square root of d to produce raw attention scores vector S_l , as shown in Fig. 2(a). Therefore, the softmax function is applied to such scores, computing the attention weights matrix A_l , as follows:

$$S_l = \frac{Q_l K_l^T}{\sqrt{d}}, \quad (1)$$

$$A_l = \text{Softmax}(S_l). \quad (2)$$

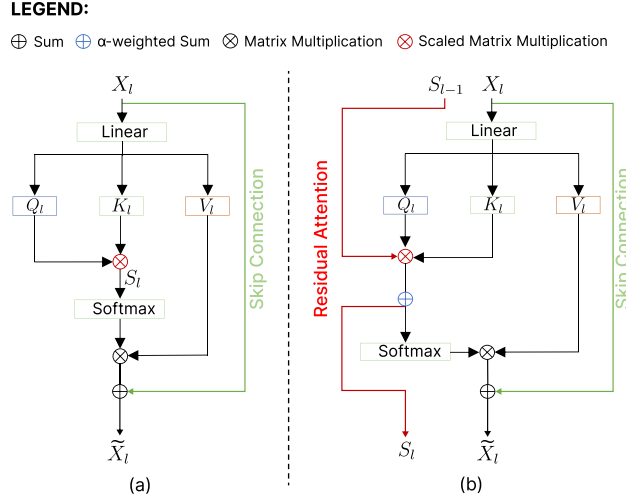


Figure 2: Illustration of the standard self-attention (a) and the proposed mechanism with residual attention module (b).

Finally, the values in V_l are scaled using the attention weights through a weighted multiplication to compute the scaled dot-product attention, defined as:

$$\tilde{X}_l = A_l V_l, \quad (3)$$

where \tilde{X}_l represents the output features of the scaled dot-product attention at layer l .

However, due to the global nature of the self-attention mechanism, processing a considerable number of patches or a big d requires a high computational cost. Therefore, Ashish et al. [34] proposed the Multi-Head Self-Attention mechanism (MHSA) to retain the computational requirements when a significant workload is required. This approach uses H different attention heads computing self-attention in different subspaces with dimension d/H derived from the Q , K , and V vectors rather than considering their full dimensionality d . In this manner, the calculations are parallelized, and the model can jointly attend to information from different representations of subspaces at different positions. Finally, the output of each head is concatenated together to obtain the final attention output. Formally, the MHSA operation is represented as:

$$MHSA(X_l) = Concat([A_{l,h} V_{l,h}]_{h=1}^H), \quad (4)$$

where h represents the head index, $A_{l,h}$ and $V_{l,h}$ are the attention weights matrix and the value vectors of head h and layer l respectively, while $Concat(\cdot)$ denotes the concatenation of the H produced feature maps along the head dimension. Consequently, \tilde{X} can now be expressed as follows:

$$\tilde{X}_l = Concat([\tilde{X}_{h,l}]_{h=1}^H), \quad (5)$$

where $\tilde{X}_{h,l}$ represents the attention scaled values at layer l and head h .

The MLP module, on the other hand, extracts features independently from each patch and is usually constructed by stacking two linear layers with parameters W_a , W_b respectively, and a non-linear activation function σ in between them. This module also represents the last processing operation of the transformer block, which takes in input \tilde{X}_l and produces the output features of layer l denoted as X_{l+1} since are going to be used as the input features for the $l + 1$ layer. Formally, it can be represented as:

$$MLP(\tilde{X}_l) = \sigma(W_{a,l} \tilde{X}_l) W_{b,l}, \quad (6)$$

where $W_{a,l}$ and $W_{b,l}$ are the weights of the two stacked linear layers composing the MLP of layer l .

3.2. Feature Collapsing

Feature collapsing is a commonly observed occurrence within ViT architectures. It refers to the phenomenon where the features extracted from different image patches lose their distinctiveness and become increasingly similar or indistinguishable as the network depth grows. This phenomenon primarily arises due to the nature of the attention

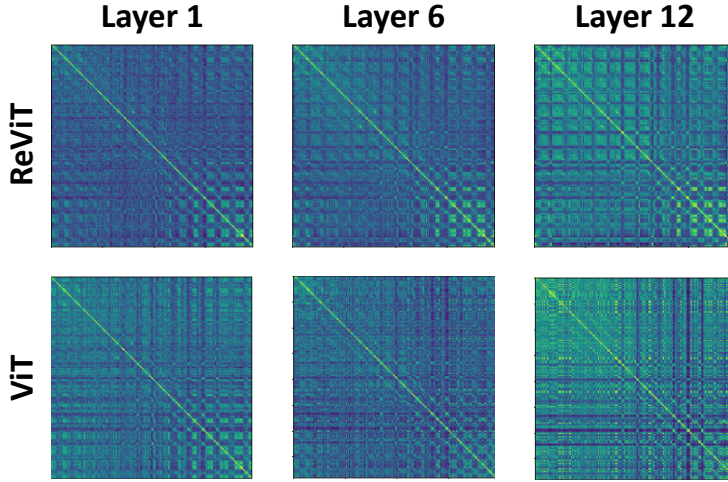


Figure 3: Feature similarity matrix in different layers for ViT and ReViT models. The color represents the similarity between each feature patch. A high frequency of green color shows high similarity between patches.

mechanism used in ViT, which progressively aggregates information from various image patches as it traverses through the network layers. Such a process can be mathematically described by representing Eq. (5) as a weighted summation of feature patches in the following manner:

$$\tilde{X}_{l,h}^i = \sum_{j=1}^N A_{l,h}^{i,j} X_{l,h}^j, \text{ subject to } \sum_{j=1}^N A_{l,h}^{i,j} = 1, \text{ for } i = [1, 2, \dots, N]. \quad (7)$$

Here, $\tilde{X}_{l,h}^i$ denotes the feature vector originating from patch i and represents a weighted average of features from all patches. The weights are determined by the values in the attention map $A_{l,h}$. Although the attention mechanism aims to capture global relationships between different feature patches [7], it can lead to the loss of feature diversity, resulting in feature collapsing. In order to provide evidence for this observation, Fig. 3 presents a visual representation of the feature similarity matrix for the ViT. This matrix is constructed by calculating the cosine similarity between distinct feature patches extracted by the ViT model. The key insight revealed by the figure is that, as the features progress from the shallower layers of the model to the deeper layers, there is a noticeable trend towards increased similarity among them.

One approach to mitigate this phenomenon is the use of residual connections, which establish connections between features across different layers while bypassing the attention mechanism. Formally, the residual connection combined with MHSA operation can be expressed as follows:

$$\text{residualMHSA}(X_l) = \text{MHSA}(X_l) + X_l. \quad (8)$$

In this equation, the identity projection X_l runs in parallel to the MHSA operation. Intuitively, because the features in X_l exhibit greater diversity before passing through the MHSA operation, the summation of the two feature vectors preserves the characteristics from the previous layer. Consequently, the output retains more diverse features. Empirical evidence supporting this phenomenon can be found in [32]. Drawing inspiration from these discoveries, this study introduces a novel approach to tackling this issue. Specifically, it suggests an innovative alternative residual connection between attention layers (without bypassing the attention mechanism) designed to curb the rapid expansion of the attention across the head dimension, which is the main source of feature collapsing, and increase feature diversity as shown in Fig. 3.

3.3. Residual Attention

Generally, ViT model customization involves modifying the MHSA mechanism, normalization layers, MLP component, or residual connections among features, maintaining a specific information flow at the feature level

Residual Attention for Vision Transformers

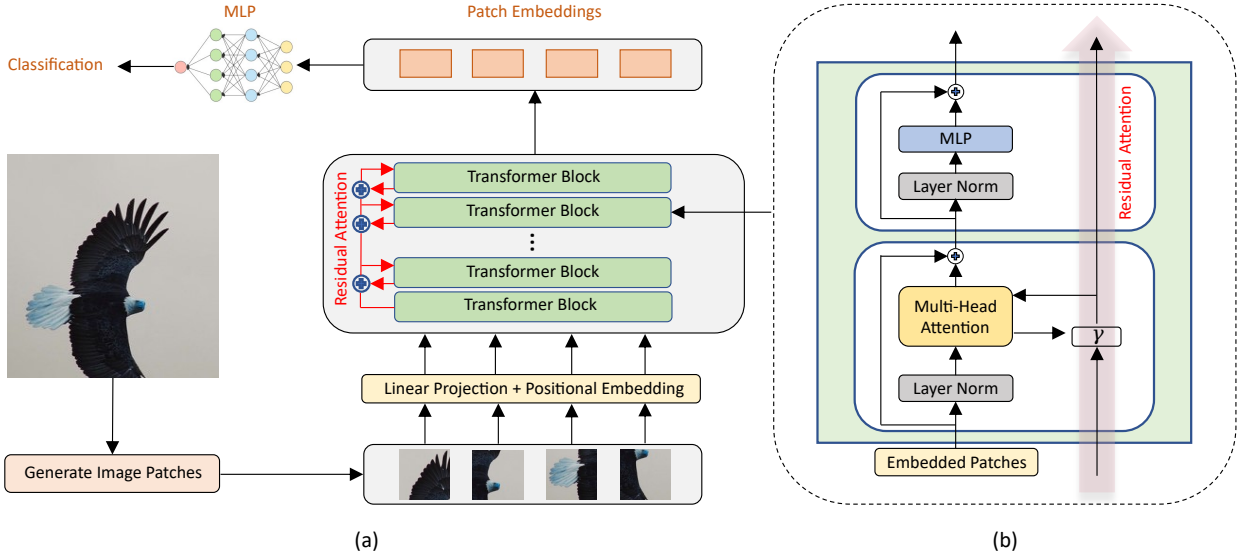


Figure 4: Illustration of the proposed ReViT network with residual attention. In (a) the overall architecture, in (b) the transformer block in detail, including the residual attention module.

between adjacent transformer blocks [7, 24]. Aiming to expand such a flow to improve the feature diversity, the ReViT architecture shown in Fig. 4(a) incorporates a novel skip connection between consecutive MHSA layers, enabling the propagation and accumulation of attention from shallow to deeper layers, as depicted in Fig. 4(b). This expansion, representing the proposed residual attention, is a complementary process to residual connections at the end of each transformer block. Indeed, while existing skip connections propagate the low-level features to deeper layers bypassing the MHSA layer, the residual attention propagates the information from Q and K , which defines the relationships between patches used to extract these features, thus enabling a new attention capability to consider previously extracted relationships while learning to extract new ones. Formally, the proposed attention mechanism is implemented by changing the computation of the S_l matrix defined in Eq. (1). Specifically, the equation is extended with an additional term representing the Q and K of the previous MHSA layers aggregated with those of the current layer, as follows:

$$S_l = \begin{cases} \frac{Q_0 K_0^T}{\sqrt{d_0}}, & \text{if } l = 0 \\ \gamma\left(\frac{Q_l K_l^T}{\sqrt{d_l}}, S_{l-1}\right), & \text{otherwise} \end{cases}, \quad (9)$$

where l indicates the l -th attention layer and γ is the permutation invariant aggregation function. For $l = 0$, the attention is computed as defined in Eq. (1). Otherwise, for $l > 0$, S_l is obtained as the γ of S_{l-1} and the scaled dot product of Q_l and K_l . Following this rationale, the information flow among adjacent MHSA layers is extended beyond the standard flow, which is limited only to feature forwarding, propagating the attention used to aggregate information between patches in previous layers. However, propagating and accumulating such information may prevent the network from learning high-level representations while amplifying the attention related to low-level features. To avoid this, γ is implemented as a weighted sum where a learnable gate variable α is introduced to allow the network to autonomously determine how much attention to propagate between layers. Precisely, α balances the quantity of residual attention transmitted from the previous to the current MHSA layer during aggregation. Formally, the Eq. (9) is further extended as follows:

$$S_l = \begin{cases} \frac{Q_l \cdot K_l^T}{\sqrt{d_l}}, & \text{if } l = 0 \\ \alpha\left(\frac{Q_l \cdot K_l^T}{\sqrt{d_l}}\right) + (1 - \alpha)(S_{l-1}), & \text{otherwise} \end{cases}, \quad (10)$$

where $\alpha \in]0; 1[$. After obtaining the balanced attention scores S_l , following Eq. (2), the softmax function is applied to compute the attention weights A_l required for obtaining the new scaled dot-product attention output, as depicted

in Fig. 2(b). Given the implementation of residual attention, it can be easily included in both existing single-scale or multi-scale vision transformer architectures, maintaining a similar computational cost.

3.4. Attention Globality

Attention globality is a concept that reflects the capacity of the attention mechanism to encompass and consider information from all patches across an image rather than being restricted to local or nearby elements. This capability becomes particularly pronounced in the deeper layers of a ViT because these layers can extract high-level representations that account for long-range relationships between patches. To quantify the globality of the attention mechanism across both heads and layers, researchers in [8] introduce a metric known as the non-locality metric. This metric calculates, for each query patch i , the relative positional distances to all key patches j weighted by their attention scores $A_{l,h}^{i,j}$. The resulting sum is then averaged by the number of patches to derive the non-locality metric for a specific head h . This can further be averaged across attention heads to obtain the non-locality metric for the entire layer. Mathematically, this metric is defined as follows:

$$D_{l,h} = \frac{1}{N} \sum_{i,j} A_{l,h}^{i,j} \|\delta^{i,j}\|, D_l = \frac{1}{H} \sum_h D_{l,h}. \quad (11)$$

Here, $\|\delta^{i,j}\|$ represents the relative positional distance between query patch i and key patch j , $D_{l,h}$ denotes the non-locality metric within a given layer l and head h , while D_l represents $D_{l,h}$ averaged along the head dimension. Moreover, since $\|\delta^{i,j}\|$ remains constant throughout the network (i.e., the relative positions of patches do not change), the value of $D_{l,h}$ relies entirely on $A_{l,h}$. Furthermore, as the non-locality metric D increases in deeper layers (indicating a shift towards global attention), it suggests that the attention matrix $A_{l,h}$ (consequently A_l) in these layers generally has a greater capacity to capture global relationships across the different attention heads compared to attention matrix from the previous layer. This property of the attention mechanism can be harnessed to demonstrate the advantages of employing residual attention in slowing down the process of globalizing A_l . Taking into account Eq. (10), which defines the calculation of A_l with a residual connection, it considers attention scores not only from the current layer l but also from previous layers. Consequently, the globality of layer l in ReViT, at a given head, can be represented as:

$$D_{l,h} = \frac{1}{N} \sum_{i,j} [\alpha(A_{l,h}^{i,j}) + (1 - \alpha)(A_{l-1,h}^{i,j})] \|\delta^{i,j}\|. \quad (12)$$

From a theoretical point of view, thanks to the above equation, given that the attention scores from earlier layers (A_{l-1}) generally tend to be more locally focused compared to those of the current layer l , the weighted combination of these sets of scores is expected to result in an attention matrix that exhibits less globality than if only the scores from the current layer were used. In other words, combining attention scores of given layer l with those of previous layers through residual attention at each head h , slows down the globalization process. For empirical proof, refer to section 4.4.

4. Experiments

In this section, we present the implementation details of the proposed method and tests conducted on some challenging datasets for image classification, object detection, and instance segmentation. In particular, we start by giving the implementation details of our method in various settings. Subsequently, we report the test results on five image classification benchmarks, namely ImageNet1K, CIFAR-10, CIFAR-100, Oxford Flowers-102, and Oxford-IIIT Pet. To proceed, the test results under position and scale changes (i.e., translation invariance) on Oxford Flowers-102 and Oxford-IIIT Pet datasets are reported. Such datasets were chosen for translation invariance testing due to their higher quality, which helps preserve important information even after applying translation transformations like scale reduction. Moreover, we investigate the attention mechanism of the networks trained on ImageNet1K, both quantitatively using the non-locality metric defined in Eq. (11-12) and qualitatively comparing the learned feature maps extracted with the GradCAM algorithm between the proposed approach and the standard ViT. Furthermore, we report the test results that show the effectiveness of our method when implemented on top of spatial-aware multiscale architectures like Swin and MViTv2 on downstream tasks like object detection and instance segmentation on the COCO2017 dataset.

4.1. Implementation Details

The proposed ReViT method is implemented as an augmented version of the standard ViT architecture. Specifically, we integrate the residual attention module on top of the standard ViT implementation using the PyTorch framework. Regarding the network version used in this study, we only relied on the base version of ViT containing 12 layers and denominated as ViT-B. To this end, we name our network ReViT-B. Additionally, as mentioned above, we conduct experiments that test the effectiveness of our method applied in the multiscale architectures, namely MViTv2 and Swin. To implement such networks, we start from their official PyTorch implementations and extend them with our module. Moreover, for MViTv2 and Swin, we exploit their tiny versions, i.e., MViTv2-T and Swin-T with 12 layers each, and name our implementations ReMViTv2-T and ReSwin-T. The rationale behind using the smaller versions of each network is that they require less computational resources, and usually, the bigger versions require pre-training on large-scale datasets like ImageNet21K or even bigger ones.

To train our networks, we use the same configurations reported in their official studies and run the experiments on an NVIDIA V100 GPU with 32GB of RAM. Specifically, for image classification on ImageNet1K, all models were trained for 300 epochs, with an input image size of 224×224 , using gradient clipping and cosine scheduling learning rate warmup/decay. For the ReViT-B network training, Adam [17] was used as optimizer with a base learning rate set to 0.001, 30 warmup epochs, an effective batch size of 4096, and the weight decay set to 0.3. Instead, for ReSwin-T model training, AdamW optimizer [26] was used by setting a base learning rate to 0.001, 20 warmup epochs, an effective batch size of 1024, and the weight decay set to 0.05. Finally, the remaining ReMViTv2-T network training was performed using the AdamW optimizer with a base learning rate set to 0.002, 70 warmup epochs, an effective batch size of 2048, and the weight decay set to 0.1. Regarding other image classification tasks, we use the same training setups reported in [7] for a fair comparison. Moreover, regarding the object detection and instance segmentation tasks, since such tasks require local awareness of features, the experiments were performed only using ReSwin-T and ReMViTv2-T. These models were trained for 36 epochs using AdamW as an optimizer and linear scheduling learning rate decay. For ReSwin-T network training, the initial learning rate was set to 0.0001, with a weight decay of 0.05, and a batch size set to 16. Instead, for ReMViTv2-T model training, the initial learning rate was set to 0.00016, with a weight decay of 0.1, and a batch size set to 64.

4.2. Image classification

For the image classification tasks, models were primarily evaluated on ImageNet1K, considered as one of the most significant benchmarks. To evaluate the performance of the models, we used the top-1 single crop accuracy metric and reported the obtained results in Table 1. As can be noticed, all models incorporating the residual attention module outperform their original network counterparts in the used metric. Specifically, ReViT-B, ReMViTv2-T, and ReSwin-T models with residual attention obtain an improvement of 4.6%, 0.4%, and 0.2%, respectively, compared to their original counterparts. Notably, ReViT-B shows a significant improvement compared to ViT-B, indicating that residual attention is more effective in single-scale architectures that employ only global attention. This is because such a module was invented to contrast the over-globalization of the attention mechanism, a phenomenon manifested in the ViT-B architecture. On the contrary, multiscale architectures like Swin-T and MViTv2-T have their own in-built local mechanisms that help preserve the low-level features throughout the network. As such, the effect of the residual attention in these networks, i.e., ReSwin-T and ReMViTv2-T, is lower but still bolsters their representational ability and achieves improved performances compared to the original counterparts. Apart from the performance enhancements, another compelling factor highlighting the significance of residual attention within single-scale architectures is the parameter α . Notably, in ReViT-B, α assumes a considerably smaller value when compared with the values observed in ReSwin-T and ReMViTv2-T. As Eq. (10) indicates, this discrepancy signifies that prior attention holds substantially more significance in the context of ReViT. Additionally, Table 2 provides a more extensive comparison with the state of the art, showing that models with residual attention perform even more comparatively to the best models.

Subsequently, ReViT-B was tested on multiple image classification benchmarks, including CIFAR-10, CIFAR-100, Oxford Flowers-102, and Oxford-IIIT Pet. The performance of ReViT-B is then compared with that of the ViT-B model, and the results are presented in Table 3. Notably, ReViT-B, with the residual attention, consistently outperforms ViT-B across all datasets with a minimum improvement of 0.6% in CIFAR10 and a maximum of 3.4% in CIFAR100. This improvement can be attributed to the residual attention module's ability to capture a wider range of visual features, thus enhancing the network's capability to distinguish between different classes based on the image content. The other models were not tested on these datasets because their official studies do not provide experimental results and focus only on large-scale datasets.

Model	Image size	Params(M)	FLOPs(G)	top-1 acc. %	α
ViT-B [7]	224 × 224	86	17.5	77.8	-
ReViT-B	224 × 224	86	17.5	82.4	0.56
Swin-T [24]	224 × 224	29	4.5	81.3	-
ReSwin-T	224 × 224	29	4.5	81.5	0.99
MViTv2-T [20]	224 × 224	24	4.7	82.3	-
ReMViTv2-T	224 × 224	24	4.7	82.7	0.99

Table 1

Performance of ViT-based state-of-the-art models with and without residual attention on ImageNet1k single-crop top-1 accuracy. In addition, image size, model parameters in millions, i.e., Params(M), models throughput measured in theoretical floating point operations per second, i.e., FLOPs(G) [7], and the final value of α are reported.

Model	Params(M)	FLOPs(G)	top-1 acc. %
ViT-B [7]	86	17.5	77.8
DeiT-B [33]	86	17.5	81.8
ConViT-B [8]	86	17.5	82.4
AugViT-B [32]	86.5	17.5	82.4
ReViT-B	86	17.5	82.4
Swin-T [24]	29	4.5	81.3
TNT-S [12]	24	5.2	81.5
CoAtNet-0 [6]	25	4.0	81.6
T2T-ViT-14 [40]	22	4.8	81.5
T2T-ViT-14 _t [40]	22	6.1	81.7
ConvNeXt-T [25]	29	4.5	82.1
MViTv2-T [20]	24	4.7	82.3
VOLO-D1 [41]	27	7.1	84.2
ReSwin-T	29	4.5	81.5
ReMViTv2-T	24	4.7	82.7

Table 2

Comparison with state-of-the-art models on ImageNet1K using input images of size 224 × 224. In addition, information about model parameters in millions and throughput measured in floating point operations per second are reported.

Model	CIFAR-10	CIFAR-100	Oxford-Flowers 102	Oxford-IIIT Pet
ViT-B [7]	98.1	87.1	89.5	93.8
ReViT-B	98.7	90.5	91.1	94.9

Table 3

Top-1 accuracy performance comparison of ViT-B and ReViT-B on CIFAR-10, CIFAR-100, Oxford-Flowers 102, and Oxford-IIIT Pet datasets.

4.3. Translation Invariance

In this study, the datasets used for visual recognition typically feature the object of interest centered within the image. This is in stark contrast to real-world scenarios where objects can be situated anywhere within the scene. To assess ReViT robustness, two experiments were devised to simulate varying scales and positions of the target object within the images as shown in Fig. 5. The performance of ReViT-B and ViT-B on the Oxford Flowers-102 and Oxford-IIIT Pet datasets are compared in these experiments.

The first experiment evaluates the models' ability to handle horizontal and vertical translations. To achieve this, the input images are horizontally and vertically shifted on the image plane by {15, 30, 45, 60}% of pixels, with the empty areas filled with zeros to maintain the same input image size as shown in Fig. 5(a) and (b). As indicated in Table 4 and Fig. 6(a), both models exhibit a similar and impressive level of horizontal translation invariance, with only a minor reduction in performance. Overall, ReViT-B demonstrates slightly superior horizontal translation invariance, especially at the 60% translation level. For the Oxford Flowers-102 dataset, ReViT-B performance decreases by 2.9% less than ViT-B at a 60% translation, while for the Oxford-IIIT Pet dataset, the decrease is 1.0% less. Similar trends

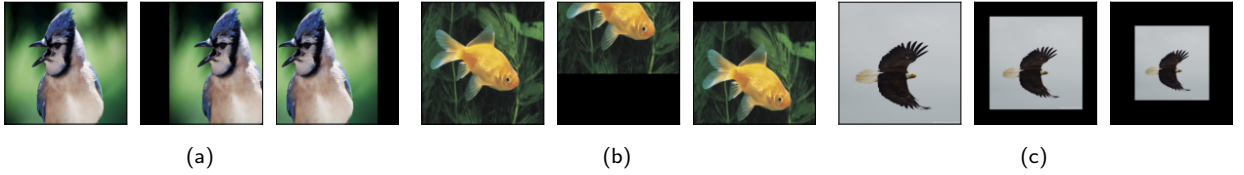


Figure 5: Visualization of transformations showcasing translation invariance, specifically horizontal shifting (a), vertical shifting (b), and changes in scale (c).

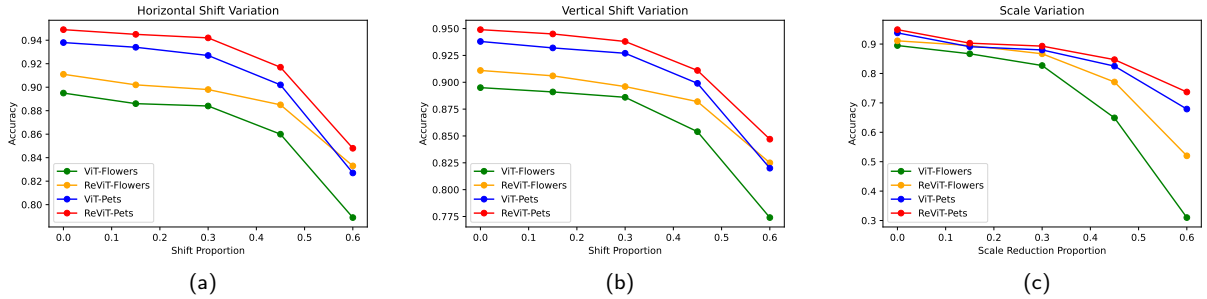


Figure 6: Translation invariance test. The graphics depict how ViT-B and ReViT-B perform when subjected to variations in horizontal shifting (a), vertical shifting (b), and changes in size (c) on the Oxford Flowers-102 and Oxford-IIT Pet datasets.

		Horizontal Translation							
		Oxford Flowers-102				Oxford-IIIT Pet			
Model		15%	30%	45%	60%	15%	30%	45%	60%
ViT-B		0.9	1.1	3.5	10.6	0.4	1.1	3.6	11.1
ReViT-B		0.8	1.2	2.5	7.7	0.4	0.7	3.2	10.1
Δ		0.1	-0.1	1.0	2.9	0.0	0.4	0.4	1.0

Table 4

Reduction in performance (in %) observed when applying a horizontal translation to input images in the Oxford Flowers-102 and Oxford-IIIT Pet datasets. Δ represents the variance in the extent of performance degradation between ReViT-B and ViT-B.

are observed for vertical translation invariance, as illustrated in Table 5 and Fig. 6(b). Although both models show a comparable drop in performance, ReViT-B displays better overall vertical translation invariance, particularly on the Oxford Flowers-102 dataset, where its performance decreases by 3.6% less than ViT-B.

In the second experiment, the scale invariance of both models is evaluated, and the results are presented in Table 6 and Fig. 6(c). To generate images at different scales, the original images are resized by reducing their width and height by {15, 30, 45, 60}%, with zero-padding to maintain the correct input size as illustrated in Fig. 5(c). Unlike the first experiment, ReViT-B consistently outperforms ViT-B in terms of scale invariance. In the case of the Oxford Flowers-102 dataset, ReViT-B shows up to 19.5% less reduction in performance accuracy, while for the Oxford-IIIT Pet dataset, it exhibits up to 4.7% less decrease than ViT-B. These results highlight that ReViT-B possesses significantly better scale invariance compared to ViT-B.

4.4. Residual Attention and Globality

The investigation into the global reach of MHSA within vision transformers, both with and without residual attention, aims to examine the hypothesis that residual attention decelerates the globalization of the attention mechanism. To assess this hypothesis quantitatively, we employ the non-locality metric calculated according to Eq. (11). Additionally, the metric is computed at both the head and layer levels. The results of this analysis, depicted in

Vertical Translation									
Model	Oxford Flowers-102				Oxford-IIIT Pet				
	15%	30%	45%	60%	15%	30%	45%	60%	
ViT-B	0.4	0.9	4.1	12.1	0.6	1.1	3.9	11.8	
ReViT-B	0.4	1.4	3.0	8.5	0.4	1.1	3.8	10.2	
Δ	0.0	-0.5	1.1	3.6	0.2	0.0	0.1	1.6	

Table 5

Diminished performance (in %) resulting from a vertical translation applied to input images within the Oxford Flowers-102 and Oxford-IIIT Pet datasets. The symbol Δ indicates the difference in performance reduction between ReViT-B and ViT-B.

Scale Variance									
Model	Oxford Flowers-102				Oxford-IIIT Pet				
	15%	30%	45%	60%	15%	30%	45%	60%	
ViT-B	2.8	6.8	24.6	58.5	0.4	1.5	7.0	25.9	
ReViT-B	1.5	4.3	13.9	39.0	0.4	1.4	6.0	21.2	
Δ	1.3	2.5	9.7	19.5	0.0	0.1	1.0	4.7	

Table 6

Diminished performance (in %) resulting from variations in scale applied to input images within the Oxford Flowers-102 and Oxford-IIIT Pet datasets. Δ indicates the disparity in performance decline between ReViT-B and ViT-B.

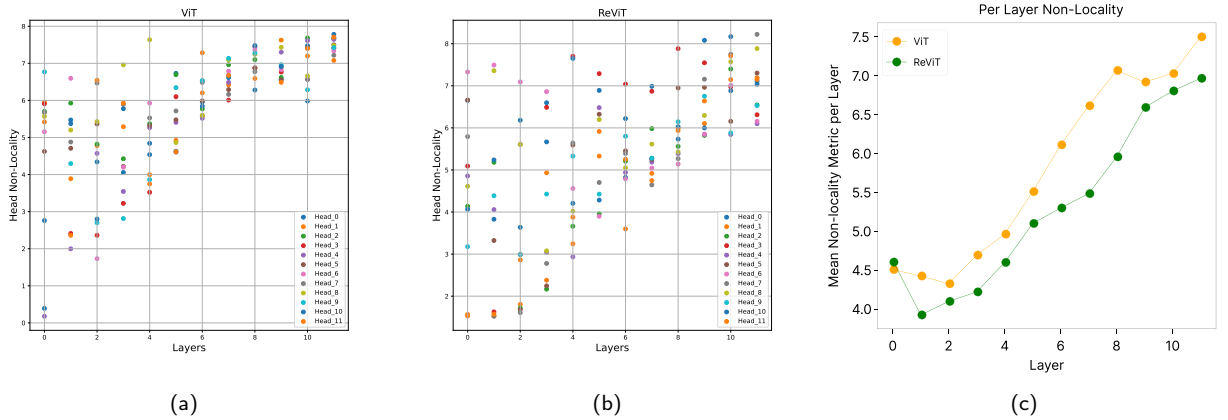


Figure 7: The non-locality metric is depicted for individual heads across all layers in the case of ViT-B in (a) and ReViT-B in (b). This visualization illustrates how the receptive field of each head expands as it progresses through deeper layers. On the other hand, in (c), a comparison of the non-locality metric between ViT-B and ReViT-B for each layer is illustrated.

Fig. 7, display the average metric across 256 input images from the ImageNet1K validation set for ViT-B and ReViT-B models trained on the same dataset. The x-axis on the plots corresponds to the layer index, while the mean non-locality for each head or layer is represented on the y-axis. Fig. 7(a) illustrates that in ViT-B, the non-locality of each head increases as it delves deeper into the layers, approaching globality which corresponds to the findings in [7, 8]. A similar trend is observed in ReViT-B, as seen in Fig. 7(b), albeit with some noteworthy distinctions. Notably, ViT-B exhibits a more consistent and monotonic increase in non-locality, with minimal variations between different heads, particularly after layer 5. In contrast, ReViT-B displays more diverse differences between heads, with some heads finding difficulty in escaping the locality while others become completely global, resulting in a less monotonic increase in non-locality. In summary, the results substantiate the hypothesis that the attention receptive field of heads in vision transformers becomes global in deeper layers, a phenomenon observed in both ViT-B and ReViT-B models. However, these findings also reveal that ReViT-B retains the ability to extract global relationships in deeper layers while still maintaining some heads that remain localized with relatively low non-locality values. Simultaneously, ViT-B is confined solely to global

relationships, leading to feature collapse. To provide a broader perspective, Fig. 7(c) presents the non-locality of ViT-B and ReViT-B at the layer level, represented as the average non-locality metric across all heads within each layer. It is evident that when computed using the same 256 input examples, ReViT-B consistently maintains lower non-locality values (except the first), indicating its ability to incorporate low-level features, with the help of relatively local heads, into the representations learned from heads that exhibit non-locality escape (i.e., become global).

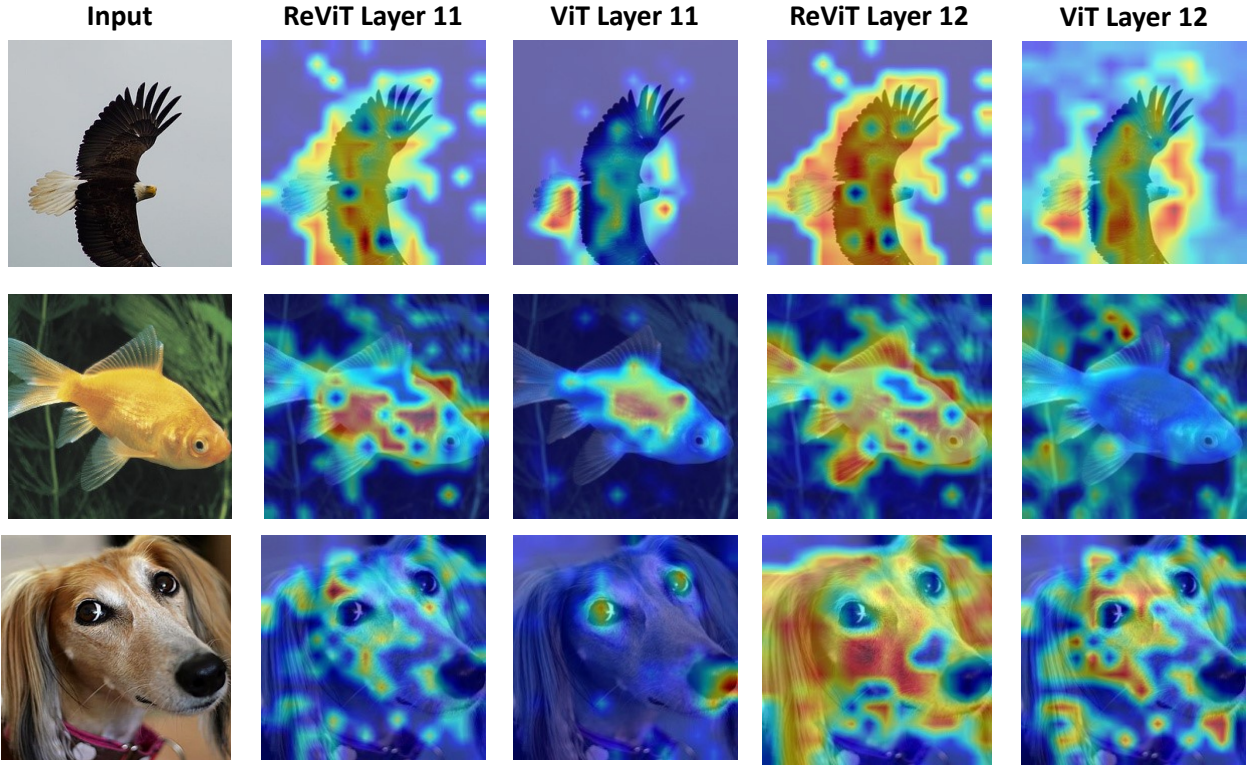


Figure 8: Comparison of feature maps in the last two layers of ViT-B and ReViT-B extracted using GradCAM algorithm from the illustrated input images.

4.5. Qualitative Comparisons

The effectiveness of the proposed residual attention module is further demonstrated through a qualitative evaluation of the features learned by ViT-B and ReViT-B using the MHSA mechanism, both with and without residual attention, respectively. To enable such a comparison, we employ the GradCAM algorithm and apply it to the last two MHSA layers of ViT-B and ReViT-B trained on ImageNet1k with samples from the validation set of the same dataset. It's worth emphasizing that layers 11 and 12 were selected due to their high globality, aligning with the objective of this experiment, which is to highlight how ReViT-B incorporates low-level features into its learned representations compared to ViT-B. To proceed, the feature maps of both models and the input images used to obtain such features are illustrated in Fig. 8. As can be noticed, the feature maps extracted from ViT-B are poor in details and lack the presence of low-level features like shapes and edges. This is caused by the globalization of its attention mechanism, which provokes the feature collapsing phenomenon. This also proves the observation made by authors in [8], which states that ViT-based architectures relying on the standard MHSA often exhibit limited attention variability, resulting in reduced feature diversity or even feature collapse [32]. On the contrary, ReViT-B, equipped with residual attention, displays greater feature diversity with feature maps almost completely aligned with the entire region where the object of interest is located, preserving the same shape. This phenomenon suggests that ReViT-B can incorporate low-level information like shapes and edges with the global context of the scene. Additionally, such ability can be attributed to residual attention. Thanks to this mechanism, the network can propagate attention maps from shallow layers to deeper layers, slowing down the globalization of attention, improving feature diversity, and incorporating low-level characteristics

Framework	Backbone	AP_{box}	AP_{box}^{50}	AP_{box}^{75}	AP_{mask}	AP_{mask}^{50}	AP_{mask}^{75}	#Params
Cascade Mask	Swin-T [24]	50.5	69.3	54.9	43.7	66.6	47.1	86M
R-CNN	ReSwin-T	50.6	69.7	54.9	43.9	66.8	47.6	86M
Mask	MViTv2-T [20]	48.2	70.9	53.3	43.8	67.9	47.2	44M
R-CNN	ReMViTv2-T	48.5	71.0	53.5	44.0	68.3	47.3	44M

Table 7

Performance of the residual attention module implemented on top of Swin and MViTv2 architectures for object detection and instance segmentation on COCO2017 5K validation set.

into the global context. Notably, this augmented feature diversity aligns with ReViT’s improved performance in terms of image classification accuracy compared to the standard ViT architecture.

4.6. Object Detection and Instance Segmentation

To assess the general applicability of the residual attention module, we test its knowledge transfer ability in downstream tasks. As such, further experiments were conducted on spatial-aware networks, i.e., ReSwin-T and ReMViTv2-T, for the tasks of object detection and instance segmentation, achieving increased results. The evaluation was performed on the COCO2017 dataset for both tasks using the COCO average precision (AP) metric, and the input images were resized with $480 \leq H \leq 800$ and $W = 1333$. For fair comparisons with the solutions proposed in [24] and [20], the Cascade Mask-RCNN [3] and the Mask R-CNN [13] models were used with the ReSwin-T and ReMViTv2-T as backbones, respectively. Additionally, both ReSwin-T and ReMViTv2-T were initialized with the weights learned during ImageNet1K training, hence, knowledge transferring. Table 7 summarizes results on the subset of 5000 validation images. For the object detection task, the ReSwin-T model performance is higher for AP_{box} and AP_{box}^{50} with respect to the original Swin-T architecture. Regarding the ReMViTv2-T model, the performance improves for all the considered APs compared to the original MViTv2-T architecture. For the instance segmentation task, ReSwin-T and ReMViTv2-T with residual attention increase the overall performance in all the metrics compared to their original works, even though by a small margin.

5. Ablation Study

In this section, we perform an ablation study to determine the significance of balancing the past and current attention information in the proposed residual attention. We will specifically examine the impact of α on various image classification benchmarks including CIFAR10, CIFAR100, Oxford Flowers-102, and Oxford-IIIT Pet.

5.1. Inspecting the effect of α

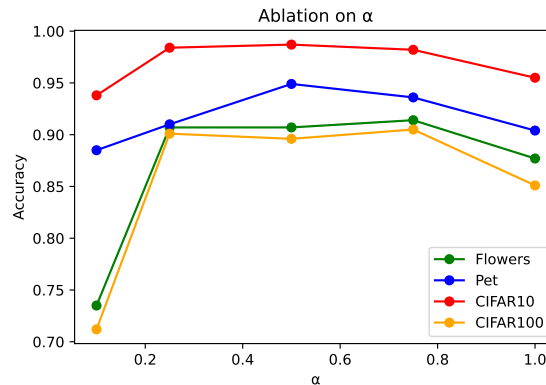


Figure 9: ReViT classification performance on CIFAR10, CIFAR100, Oxford Flowers-102 and Oxford-IIIT Pet datasets for different values of α .

The notion of residual attention acts as a conduit for propagating attention information through diverse layers via a shortcut connection, formally represented in Eq. (10). Introducing a trainable gate variable, denoted as α , ensures a

balanced incorporation of residual attention information within this connection. The pivotal role of α lies in its ability to regulate past and present information flow, maintaining a harmonious equilibrium. A meticulous series of experiments are devised to study this variable's impact empirically.

These experiments encompass an assessment of ReViT's performance in classification tasks, with the gating variable held constant while manually adjusting its values to observe the model's behavior. Specifically, ReViT is tested across four classification benchmarks: CIFAR10, CIFAR100, Oxford Flowers-102, and Oxford-IIIT Pet, with α values spanning from 0 to 1. With 0 being the lower extremity considering only past attention and 1 being the other extremity completely ignoring past attention (i.e., ViT). The outcomes of these experiments are graphically presented in Fig. 9. For $\alpha = 0$, according to Eq. (10), ReViT relies only on the attention information from the first layer, and as expected, the performance decreases, especially on complex datasets like CIFAR100 and Oxford Flowers-102. Such performance collapse is explained by the fact that for an $\alpha = 0$, ReViT lacks global context. For the other values of α , notably, in datasets characterized by a modest number of classes and a surplus of examples per class, such as CIFAR10, the impact is relatively subdued. However, in a more demanding dataset featuring significant inter-class and intra-class variations compared to CIFAR10, like Oxford-IIIT Pet, the role of α becomes more pivotal, exemplified by the model's sensitivity to varying α values affecting its performance. Furthermore, in datasets like CIFAR100 and Oxford Flowers-102, which are even more complex, the effect of α on ReViT becomes even more important and manifests quite similarly with the model attaining peak performance at $\alpha = 0.75$, and experiencing a sharp decline as it approaches 1. Considering that an α value close to 1 typically does not yield the optimal performance across all datasets, it becomes evident that past attention information is crucial for learning better representation, and α assumes a vital role within ReViT. It balances the integration of past and current attention information, facilitating the extraction of high-quality image representations encompassing high and low-level features.

6. Conclusion

In this study, we introduce the innovative Residual Attention Vision Transformer (ReViT) network, which integrates residual attention learning to enhance the extraction of visual features in Vision Transformer (ViT) architectures. The proposed approach effectively transmits and accumulates attention information from queries and keys across successive Multi-Head Self-Attention (MHSA) layers. Such residual connection prevents diminishing low-level visual features. Additionally, it empowers the model to leverage previously extracted features while learning new ones by decelerating the over-globalization of the attention mechanism. The efficacy and robustness of the proposed methods are evaluated on five popular image classification benchmarks, including ImageNet1K, CIFAR-10, CIFAR-100, Oxford Flowers-102, and Oxford-IIIT Pet, as well as the COCO2017 dataset for object detection and instance segmentation. The results demonstrate that residual attention learning elevates the performance of ViT-based neural models in visual recognition tasks. Furthermore, it adeptly preserves and enhances the ability to uncover and incorporate semantic and spatial relationships when integrated into spatial-aware neural networks, facilitating the identification, localization, and segmentation of individual objects within an image. However, since the introduced residual module contrasts the globalization of the attention mechanism, its efficacy is limited when applied in multi-scale architectures with local awareness, providing less improvement compared to its application in single-scale architecture with global attention. Motivated by such limitations, in future works, refining the residual attention module to better suit multi-scale transformer architectures could provide further insights into its effectiveness in such architectures.

Acknowledgements

This work was supported by "Smart unmannEd AeRial vehiCles for Human likE monitoRing (SEARCHER)" project of the Italian Ministry of Defence within the PNRM 2020 Program (Grant Number: PNRM a2020.231); "A Brain Computer Interface (BCI) based System for Transferring Human Emotions inside Unmanned Aerial Vehicles (UAVs)" Sapienza University Research Projects (Grant Number: RM1221816C1CF63B); "EYE-FLAI: going bEYond computEr vision paradigm using wi-FI signals in AI systems" project of the Italian Ministry of Universities and Research (MUR) within the PRIN 2022 Program (Grant Number: 2022AL45R2) (CUP: B53D23012950001); and MICS (Made in Italy – Circular and Sustainable) Extended Partnership and received funding from Next-Generation EU (Italian PNRR – M4 C2, Invest 1.3 – D.D. 1551.11-10-2022, PE00000004). CUP MICS B53C22004130001.

References

- [1] Alam, M.M., Islam, M.T., Rahman, S.M., 2022. Unified learning approach for egocentric hand gesture recognition and fingertip detection. *Pattern Recognition* 121, 108200. doi:<https://doi.org/10.1016/j.patcog.2021.108200>.
- [2] Avola, D., Bernardi, M., Cascio, M., Cinque, L., Foresti, G.L., Massaroni, C., 2019. A new descriptor for keypoint-based background modeling, in: *International Conference on Image Analysis and Processing (ICIAP)*, pp. 15–25. doi:10.1007/978-3-030-30642-7_2.
- [3] Cai, Z., Vasconcelos, N., 2018. Cascade r-cnn: Delving into high quality object detection, in: *IEEE/CVF Conference on Computer Vision and Pattern Recognition (CVPR)*, pp. 6154–6162. doi:10.1109/CVPR.2018.006644.
- [4] Chen, L., Zhou, F., Wang, S., Dong, J., Li, N., Ma, H., Wang, X., Zhou, H., 2022. Swipenet: Object detection in noisy underwater scenes. *Pattern Recognition* 132, 108926. doi:<https://doi.org/10.1016/j.patcog.2022.108926>.
- [5] Chu, X., Tian, Z., Wang, Y., Zhang, B., Ren, H., Wei, X., Xia, H., Shen, C., 2021. Twins: Revisiting the design of spatial attention in vision transformers, in: *Advances in Neural Information Processing Systems (NeurIPS)*, pp. 9355–9366.
- [6] Dai, Z., Liu, H., Le, Q.V., Tan, M., 2021. Coatnet: Marrying convolution and attention for all data sizes. *Advances in neural information processing systems* 34, 3965–3977.
- [7] Dosovitskiy, A., Beyer, L., Kolesnikov, A., Weissenborn, D., Zhai, X., Unterthiner, T., Dehghani, M., Minderer, M., Heigold, G., Gelly, S., Uszkoreit, J., Houlsby, N., 2021. An image is worth 16x16 words: Transformers for image recognition at scale, in: *International Conference on Learning Representations (ICLR)*, pp. 1–21.
- [8] d'Ascoli, S., Touvron, H., Leavitt, M.L., Morcos, A.S., Biroli, G., Sagun, L., 2021. Convit: Improving vision transformers with soft convolutional inductive biases, in: *International Conference on Machine Learning (ICML)*, pp. 2286–2296.
- [9] Gao, L., Chen, L., Liu, P., Jiang, Y., Li, Y., Ning, J., 2023. Transformer-based visual object tracking via fine-coarse concatenated attention and cross concatenated mlp. *Pattern Recognition*, 109964doi:<https://doi.org/10.1016/j.patcog.2023.109964>.
- [10] González-Díaz, I., Buso, V., Benois-Pineau, J., 2016. Perceptual modeling in the problem of active object recognition in visual scenes. *Pattern Recognition* 56, 129–141. doi:<https://doi.org/10.1016/j.patcog.2016.03.007>.
- [11] Han, K., Xiao, A., Wu, E., Guo, J., Xu, C., Wang, Y., 2021a. Transformer in transformer, in: *Advances in Neural Information Processing Systems (NeurIPS)*, pp. 15908–15919.
- [12] Han, K., Xiao, A., Wu, E., Guo, J., Xu, C., Wang, Y., 2021b. Transformer in transformer. *Advances in Neural Information Processing Systems* 34, 15908–15919.
- [13] He, K., Gkioxari, G., Dollár, P., Girshick, R., 2017. Mask r-cnn, in: *IEEE International Conference on Computer Vision (ICCV)*, pp. 2980–2988. doi:10.1109/ICCV.2017.322.
- [14] Hong, Y., Pan, H., Jia, Y., Sun, W., Gao, H., 2022. Resdnet: Efficient dense multi-scale representations with residual learning for high-level vision tasks. *IEEE Transactions on Neural Networks and Learning Systems (TNLS)*, 1–12doi:10.1109/TNNLS.2022.3169779.
- [15] Huff, T., Mahabadi, N., Tadi, P., 2022. Neuroanatomy, visual cortex, in: *StatPearls [Internet]*. StatPearls Publishing, pp. –.
- [16] Kim, B.J., Choi, H., Jang, H., Lee, D.G., Jeong, W., Kim, S.W., 2023. Improved robustness of vision transformers via prelayernorm in patch embedding. *Pattern Recognition* 141, 109659. doi:<https://doi.org/10.1016/j.patcog.2023.109659>.
- [17] Kingma, D.P., Ba, J., 2015. Adam: A method for stochastic optimization., in: *International Conference on Learning Representations (ICLR)*, pp. 1–13.
- [18] Krizhevsky, A., Hinton, G., 2009. Learning multiple layers of features from tiny images. Technical Report .
- [19] Laith, A., Jinglan, Z., Amjad J., H., Ayad, A.D., Ye, D., Omran, Al-Shamma J., S., Mohammed A., F., Muthana, A.A., Laith, F., 2021. Review of deep learning: concepts, cnn architectures, challenges, applications, future directions. *Journal of Big Data* 8, 1–74. doi:10.1186/s40537-021-00444-8.
- [20] Li, Y., Wu, C.Y., Fan, H., Mangalam, K., Xiong, B., Malik, J., Feichtenhofer, C., 2022a. Mvity2: Improved multiscale vision transformers for classification and detection, in: *IEEE/CVF Conference on Computer Vision and Pattern Recognition (CVPR)*, pp. 4794–4804. doi:10.1109/CVPR52688.2022.00476.
- [21] Li, Z., Liu, F., Yang, W., Peng, S., Zhou, J., 2022b. A survey of convolutional neural networks: Analysis, applications, and prospects. *IEEE Transactions on Neural Networks and Learning Systems (TNLS)* 33, 6999–7019. doi:10.1109/TNNLS.2021.3084827.
- [22] Lin, H., Cheng, X., Wu, X., Shen, D., 2022. Cat: Cross attention in vision transformer, in: *IEEE International Conference on Multimedia and Expo (ICME)*, pp. 1–6. doi:10.1109/ICME52920.2022.9859720.
- [23] Lin, T.Y., Maire, M., Belongie, S., Hays, J., Perona, P., Ramanan, D., Dollár, P., Zitnick, C.L., 2014. Microsoft coco: Common objects in context, in: *European Conference in Computer Vision (ECCV)*, pp. 740–755. doi:https://doi.org/10.1007/978-3-319-10602-1_48.
- [24] Liu, Z., Lin, Y., Cao, Y., Hu, H., Wei, Y., Zhang, Z., Lin, S., Guo, B., 2021. Swin transformer: Hierarchical vision transformer using shifted windows, in: *IEEE/CVF International Conference on Computer Vision (ICCV)*, pp. 9992–10002. doi:10.1109/ICCV48922.2021.00986.
- [25] Liu, Z., Mao, H., Wu, C.Y., Feichtenhofer, C., Darrell, T., Xie, S., 2022. A convnet for the 2020s, in: *Proceedings of the IEEE/CVF conference on computer vision and pattern recognition*, pp. 11976–11986.
- [26] Loshchilov, I., Hutter, F., 2019. Decoupled weight decay regularization, in: *International Conference on Learning Representations (ICLR)*, pp. 1–9.
- [27] Lowry, S., Sünderhauf, N., Newman, P., Leonard, J.J., Cox, D., Corke, P., Milford, M.J., 2016. Visual place recognition: A survey. *IEEE Transactions on Robotics* 32, 1–19. doi:10.1109/TR0.2015.2496823.
- [28] Nilsback, M.E., Zisserman, A., 2008. Automated flower classification over a large number of classes, in: *Sixth Indian Conference on Computer Vision, Graphics and Image Processing (ICVGIP)*, pp. 722–729. doi:10.1109/ICVGIP.2008.47.
- [29] Parkhi, O.M., Vedaldi, A., Zisserman, A., Jawahar, C., 2012. Cats and dogs, in: *IEEE/CVF Conference on Computer Vision and Pattern Recognition (CVPR)*, pp. 3498–3505. doi:10.1109/CVPR.2012.6248092.
- [30] Russakovsky, O., Deng, J., Su, H., Krause, J., Satheesh, S., Ma, S., Huang, Z., Karpathy, A., Khosla, A., Bernstein, M., Berg, A.C., Fei-Fei, L., 2015. Imagenet large scale visual recognition challenge. *International Journal of Computer Vision (IJCV)* 115, 211–252. doi:10.1007/s11263-015-0816-y.

- [31] Selvaraju, R.R., Cogswell, M., Das, A., Vedantam, R., Parikh, D., Batra, D., 2017. Grad-cam: Visual explanations from deep networks via gradient-based localization, in: 2017 IEEE International Conference on Computer Vision (ICCV), pp. 618–626. doi:10.1109/ICCV.2017.74.
- [32] Tang, Y., Han, K., Xu, C., Xiao, A., Deng, Y., Xu, C., Wang, Y., 2021. Augmented shortcuts for vision transformers, in: Advances in Neural Information Processing Systems (NeurIPS), pp. 15316–15327.
- [33] Touvron, H., Cord, M., Douze, M., Massa, F., Sablayrolles, A., Jegou, H., 2021. Training data-efficient image transformers & distillation through attention, in: International Conference on Machine Learning (ICML), pp. 10347–10357.
- [34] Vaswani, A., Shazeer, N., Parmar, N., Uszkoreit, J., Jones, L., Gomez, A.N., Kaiser, L., Polosukhin, I., 2017. Attention is all you need, in: Advances in Neural Information Processing Systems (NeurIPS), pp. 1–11.
- [35] Wang, F., Jiang, M., Qian, C., Yang, S., Li, C., Zhang, H., Wang, X., Tang, X., 2017. Residual attention network for image classification, in: IEEE/CVF Conference on Computer Vision and Pattern Recognition (CVPR), pp. 6450–6458. doi:10.1109/CVPR.2017.683.
- [36] Wang, P., Wang, X., Wang, F., Lin, M., Chang, S., Li, H., Jin, R., 2022. Kvt: k-nn attention for boosting vision transformers, in: European Conference in Computer Vision (ECCV), pp. 285–302. doi:https://doi.org/10.1007/978-3-031-19769-7_1.
- [37] Yin, Y., Xu, D., Wang, X., Zhang, L., 2021. Agunet: Annotation-guided u-net for fast one-shot video object segmentation. Pattern Recognition 110, 107580. doi:https://doi.org/10.1016/j.patcog.2020.107580.
- [38] Yu, T., Zhao, G., Li, P., Yu, Y., 2022. Boat: Bilateral local attention vision transformer, in: British Machine Vision Conference (BMVC), pp. 21–24.
- [39] Yuan, L., Chen, Y., Wang, T., Yu, W., Shi, Y., Jiang, Z., Tay, F.E.H., Feng, J., Yan, S., 2021a. Tokens-to-token vit: Training vision transformers from scratch on imagenet, in: IEEE/CVF International Conference on Computer Vision (ICCV), pp. 538–547. doi:10.1109/ICCV48922.2021.00060.
- [40] Yuan, L., Chen, Y., Wang, T., Yu, W., Shi, Y., Jiang, Z.H., Tay, F.E., Feng, J., Yan, S., 2021b. Tokens-to-token vit: Training vision transformers from scratch on imagenet, in: Proceedings of the IEEE/CVF international conference on computer vision, pp. 558–567.
- [41] Yuan, L., Hou, Q., Jiang, Z., Feng, J., Yan, S., 2022. Volo: Vision outlooker for visual recognition. IEEE transactions on pattern analysis and machine intelligence 45, 6575–6586.
- [42] Zheng, P., Zhao, Z.Q., Gao, J., Wu, X., 2017. Image set classification based on cooperative sparse representation. Pattern Recognition 63, 206–217. doi:https://doi.org/10.1016/j.patcog.2016.09.043.